

Drop On Demand Performance Of Polyethylene Glycol And Isopropanol Ink For Binder Jet Printing

Bupesh.M¹, Manikandan.N², Rajesh.P.K³

^{1,2,3}Department of Automobile Engineering, PSG College of Technology, Coimbatore, India.

Abstract: *In today's modern era 3D printing plays a major role in manufacturing a prototype for components that may be subjected to real-time applications. The most commonly used 3D printers are Fused Deposition Modeling (FDM) printers because of its cost and easy feed of materials in the form of the filament. On the brighter side, binder jet printing is a developing technology, which uses the principle of traditional inkjet printing. The major difference is that it applies a binder material layer by layer on a base metal powder to form a 3D object. In this paper, a binder material study suitable to have a proper homogenous formation when applied on a metal powder was performed. Both additive and binder property studies have been done and produced in this report. Five sample binder materials in different ratios were synthesized and characterized for the rheological parameters. For inkjet printability, the printable parameter "Z" should be in the range of $1 < Z < 10$. Two of the synthesized samples S1 and S5 in which the additive ratio is higher are found suitable for binder jet printing. Droplet analysis in Flow 3D was carried out to ensure the drop formation properties.*

Keywords: *Inkjet, Binder-Jet Printing, Polyethylene glycol, Iso-Propanol, Printable parameter, Reynolds number.*

1. INTRODUCTION

Additive manufacturing is the technique of gradually layering a material onto a substrate to create a 3D product[1]. Currently, the 3D printing processes in use are Fused Deposition Modelling (FDM), Stereolithography (SLA), Selective Laser Sintering (SLS), Direct Metal Laser Sintering (DMLS), Direct Metal Deposition (DMD), Direct Ink Writing (DIW), Inkjet Printing and Binder Jet Printing[2]. FDM is the leading 3D printing process used by engineers and hobbyists to get a prototype by changing the filament material[3]. Laser printing is a costly process and consumes lot of power when compared to binder jet printing which uses a simple method to bind or join the metal base using a liquid binder (e.g., water-based glycerol, Phosphoric acid, etc.) along with additive (e.g. methanol, ethanol, Isoamyl, etc.)[4]. Also, metal-based binder jet printing is an evolving technology that requires a lot of focus on additive, binder and metal-based compounds[5]. Besides metal based compounds, binder jetting is suitable for manufacturing high temperature ceramic structures[6]. The disadvantages with the conventional additive and binders are resulting poor surface finish, late drying, etc[7]. Non-homogenous spreading of the binder on the powder surface also results in dimensional inaccuracy. So, there is a need for proper formulation of binder and

additive ratios to produce 3D objects of required accuracy and surface finish. Surface roughness and other mechanical properties have to be improved in binder jet printing to make it standard for manufacturing 3D components. The current work is focused on the improvement of the binder jet process by maintaining standard viscosity, density, and surface tension of the binder material and obtain a printable parameter Z between 1 to 10.

2. MATERIALS AND METHODS

2.1 Materials used

There are multiple materials in use for additive, binder, and metal base currently, out of which polyethylene glycol and Iso-propanol are selected as the additive and binder respectively.

Polyethylene glycol (PEG) is a polymer that is obtained after the repeated addition of monomeric units named ethylene glycol ($C_2H_6O_2$). This process is called polymerization. PEG has both a linear structure and a branched (star) structure as shown in Fig 1. Since it is a polymer it has strong intermolecular forces of attraction which results in strong chemical bonds. This strong chemical bond indicated that Polyethylene glycol has good mechanical strength when used as an additive in Binder-Jet 3D Printing.

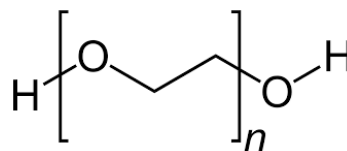


Fig. 1. Polyethylene glycol

Isopropanol is known as rubbing alcohol which has less viscosity and hence it is capable of transporting the additive selected from ink head to the nozzle very effectively by reducing the friction flow through pipes from ink head to nozzle.

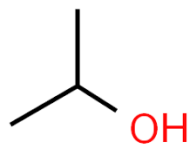


Fig. 2. Iso Propanol

The most commonly used base material is aluminium oxide nanoparticles since aluminium has been proved to be a useful material due to its lightweight, mechanical strength, stress, and strain factors[8]. Another main reason for choosing aluminium oxide nanoparticles is that when ink falls on the base metal layer, the spherical shape of aluminium oxide nanoparticles will have point contact which enhances the binder and metal base cohesion. Moreover, a proper homogenous mixture can be obtained rather than a heterogenous mixture that is formed when ceramic particles with irregular shape and size are used. This irregular shape and size form surface contact when diffused with ink which leads to the heterogenous mixture. The importance is given to homogenous mixture and point contact between base metal powder because a uniform distribution of ink can be produced.

The samples are prepared in five different ratios of additive and binder: 3:1, 1:1, 3:1,1:4 and 4:1 by using stir blending technique. The corresponding material preparation ratios are mentioned in Table 1.

Table .1 Sample ratios of additive and binder

Sample No.	Polyethylene glycol (%)	Iso-Propanol(%)	Ratio
1.	75	25	3:1
2.	50	50	1:1
3.	25	75	1:3
4.	20	80	1:4
5.	80	20	4:1

2.2 Rheological characterization

Rheological characterization is highly critical to confirm the inkjet printability of any ink. Various parameters like density, dynamic viscosity and surface tension govern the inkjet printability of an ink[9].

2.2.1 Density

A tube filled with a different liquid will have a different coefficient of expansion thereby, will rise when dipped in the liquid to be tested. This result is compared with the traditional way of measuring density which is by measuring the volume of the container and mass of the liquid to be tested.

2.2.2 Dynamic viscosity:

The internal resistance to flow of a fluid is measured by dynamic viscosity, whereas the ratio of dynamic viscosity to density is measured by kinematic viscosity. Here kinematic viscosity is measured by placing the 5 different test samples one by one in a glass tube. The values are measured by varying the time and the value is obtained in terms of centistokes (cSt). Since dynamic viscosity (Eq.1) cannot be calculated directly the kinematic viscosity has to be multiplied by specific gravity (Eq. 2) of liquid and then the dynamic viscosity is calculated from Eq.1.

$$\text{Dynamic viscosity } (\mu) = v \times S(1)$$

$$\text{Specific gravity } (S) = \frac{\text{Weight density of liquid}}{\text{Weight density of water}}(2)$$

$$\text{Kinematic viscosity} = v = \frac{\mu}{\rho}(3)$$

where,

v - Kinematic viscosity of the liquid

ρ - Density of the liquid

2.2.3 Surface tension

The meniscus method was used to determine the surface tension of the samples as given in Eq. (4).

$$\text{Surface tension } (T) = \frac{(h + \frac{r}{3})r\rho g}{2} \text{ Nm}^{-1} \quad (4)$$

where,

h – the height of liquid rise in the capillary tube (m)

r – radius of the capillary tube (m)

ρ – density of the liquid ($\frac{\text{Kg}}{\text{m}^3}$)

g – acceleration due to gravity (9.81 m/s^2).

The density, dynamic viscosity, and surface tension values that were measured are shown in Table 2.

Table – 2
 Measured density, dynamic viscosity and surface tension of the binder samples.

Sample No.	Density (Kg/m ³)	Kinematic viscosity (cSt)	Dynamic viscosity (cp)	Surface tension (N/m ²)
1	1010	4.08	4.12	0.018
2	932	1.91	1.78	0.016
3	852	1.00	0.85	0.014
4	844	0.88	0.73	0.028
5	1030	4.48	4.61	0.019

3. INKJET PRINTABILITY

3.1 Printable parameter (Z)

The rheological characterization process is followed by a study of droplet and tail formation for effective ejection of the binder from the nozzle.

The binders now in use aren't very versatile. The use of the same binder for different types of ink cannot assure enough strength and subsequent green body operations. To be printable, the binder must be designed according to particular principles: it must be able to create droplets repeatedly and routinely at a set frequency. Derby summarised these concepts, stating that the physical qualities of the fluid and the rheological properties of the binder are both important. [10].

The parameters like density, characteristic length, viscosity, Surface tension are calculated by subjecting the test samples available at different ratios in digital measuring instruments and mechanical measuring instruments. The printability of a fluid is characterized by dimensionless numbers such as Reynolds number (Re), Ohnesorge number (Oh), Weber number (We), Capillary number (Ca) and "Z"[11]. The relationship between all the dimensionless numbers are shown from Eqs. (5) to (8).

$$Re = \frac{v\rho A}{\eta} \quad (5)$$

where,

v – Velocity

ρ –Density (Kg/m³)

A – Characteristic length (Droplet diameter)

η –Dynamic viscosity(Pa-s) or poise

$$We = \frac{v^2 \rho A}{\gamma} \quad (6)$$

where,

γ –Surface Tension (N/m)

$$Oh = \frac{\sqrt{We}}{Re} = \frac{\eta}{(\gamma \rho A)^{1/2}} \quad (7)$$

The dimensionless number "Z" is given by the inverse of Ohnesorge number which describes the printability of the binder.

$$Z = \frac{1}{Oh}(8)$$

When,

- (a). Z value interval - $10 > Z > 1$ then the liquid can be printable,
- (b). when $Z < 1$, ejection of droplets is prevented by viscous forces
- (c). whereas when $Z > 10$, the ejection of the primary droplets is accompanied by the formation of a significant number of satellite droplets [12].

Besides, Derby also mentioned two further characteristics that the binder must meet in order to stabilise printing. The first need is that the droplets have a minimum speed in order to overcome surface tension and be ejected from the nozzle. The minimal velocity, which is presented below, can be used to express this speed Eq. (9).

$$\text{Minimum Velocity, } V_{\min} = \sqrt{\frac{4\gamma}{\rho d_n}}(9)$$

The capillary number (Ca) is a dimensionless variable in fluid dynamics that represents the relative effect of viscous drag forces vs surface tension forces acting across an interface between two immiscible liquids or a liquid and a gas. [13].

$$Ca = \frac{\mu * V}{\gamma} \quad (10)$$

The calculated dimensionless numbers for the five samples are shown in Table 3.

Table – 3 Calculated dimensionless numbers for the samples

Sample No.	Reynolds number (Re)	Weber's number (We)	Ohnesorg number (Oh)	(Z)	Minimum velocity (m/s)
1	98.034	112.22	0.108	9.25	1.19
2	209.43	116.50	0.052	19.40	1.17
3	400.00	121.71	0.028	36.25	1.14
4	459.94	60.28	0.017	59.23	1.62
5	89.29	108.42	0.117	8.57	1.21

3.2 Inkjet printing regimes

The five samples are plotted with each having 4 data points which are taken by varying the velocity values from 2 to 3.5 m/s with increment of 0.5 m/s.

3.2.1 Weber number Vs Reynolds number

All the samples have satellite formation because they are on the right-hand side of the boundary condition ($Z > 10$). All samples produce satellite but has sufficient energy for drop formation and does not produce splashing.

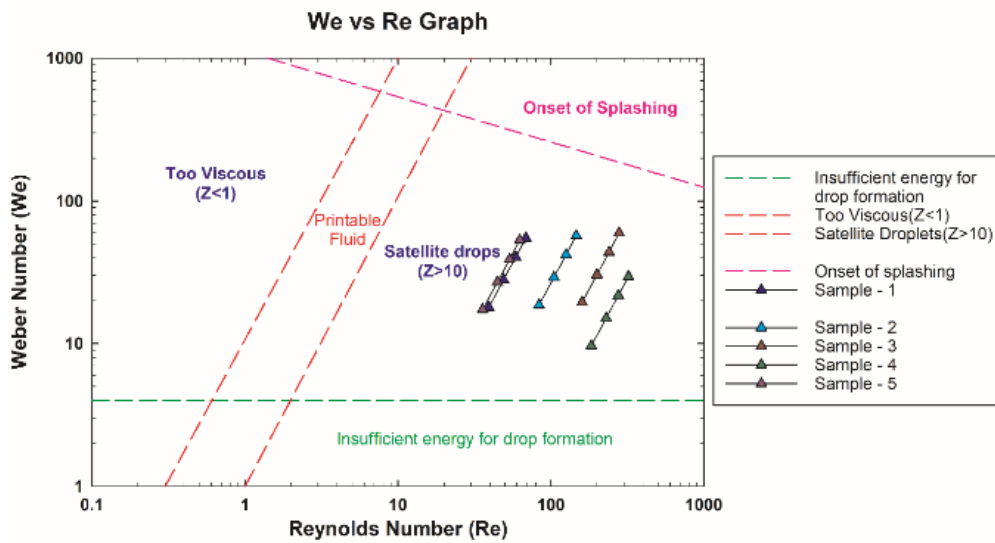


Fig.3 Weber Number Vs Reynolds number printability regime[10]

3.2.2 Weber Number Vs Z

The We-Z values if lay in the stable area the splashing will reduce which will help us to avoid the formation of objects apart from the coordinates where the necessary component have to be manufactured[11].

This is one mathematical model where the tested sample values can be compared provided that each sample has four points on the graph where the values are obtained by varying the velocity. The velocity value starts from 2 because all the minimum velocity required to overcome the surface tension for all five samples is greater than 1.147 m/s from Table – 3.

If values for velocity is less than the calculated minimum velocity from Table – 3 then the sample values lie stable region but we cannot make the fluid come out of the nozzle because the velocity will not meet the threshold value of surface tension exerted by the fluid and nozzle wall surface.

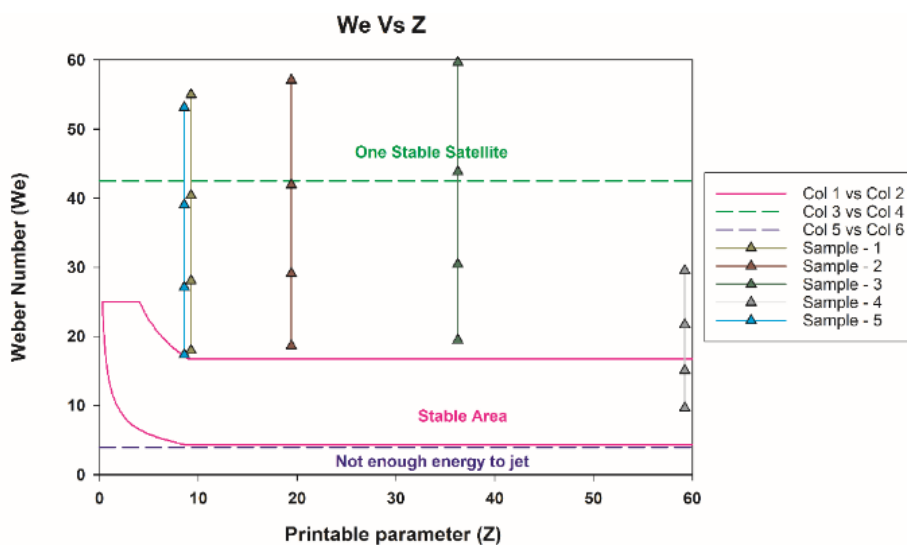


Fig.4 We vs Z printability regime [11]

Fig. 4. shows that sample four lies in a stable area with velocity values 2 and 2.5 m/s. whereas sample five lies in a stable area with a velocity value of 2 and 2.5 m/s. Provided that all the samples produce stable satellites meaning that they are very small in size and have a very small splashing effect at a velocity 3.5m/s or higher.

3.2.3 Weber number Vs Ohnesorgenumber

The pushing power for first drop spreading after impact is shown in a metre space defined by the axes of Ohnesorge and Weber's figures. The circumstances for Drop on Demand (DOD) inkjet printing are shown as a green closed boundary, showing that inertial or impact forces are responsible for the initial drop behaviour. [10].DOD refers to a type of inkjet printing technology in which drops are ejected from the printhead only when they are needed. A pressure pulse is created within the printhead, which causes the drops to form. So here sample 1 and 2 are In the DOD printing region, whereas the remaining samples are having negligible viscosity and are slightly impact-driven meaning that they produce droplets in excess quantity leading to satellite formation due to the movement of the piston which gets energy by subjecting voltage to piezo[14].

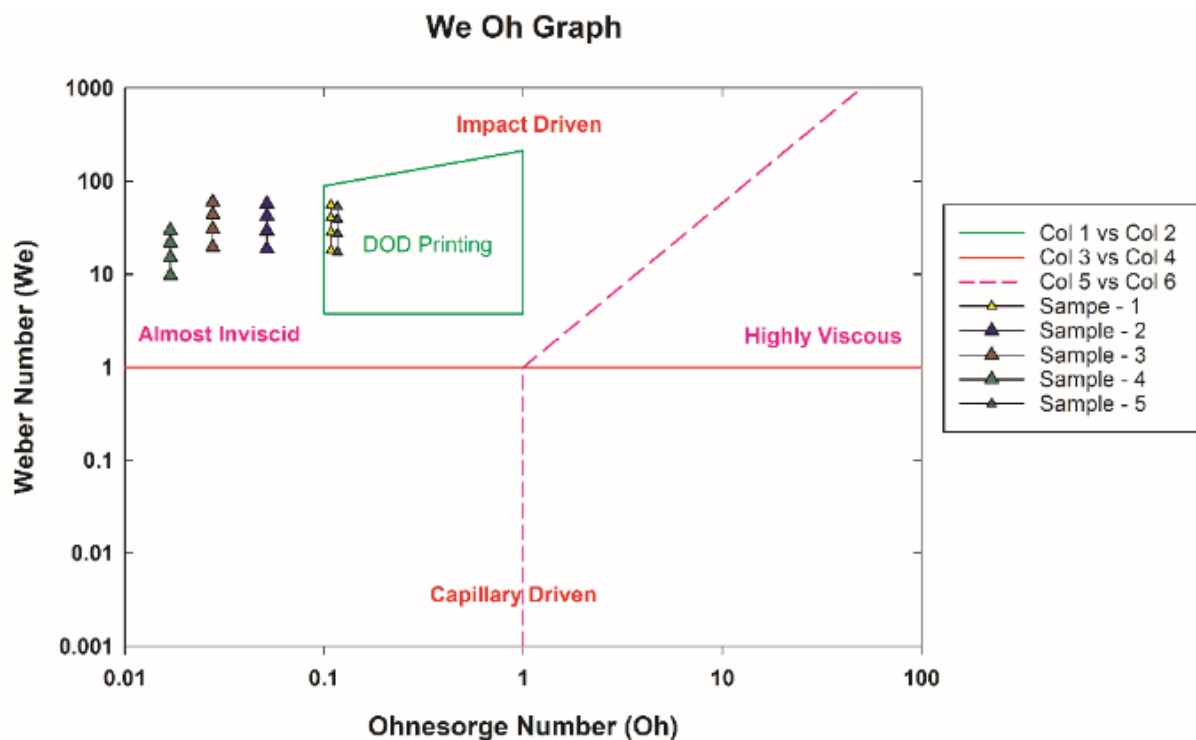


Fig. 5 We vs Oh printability regime [10]

3.2.4 Weber number Vs Ohnesorgenumber

From this comparison, sample-2 lies in the printability window very effectively. But samples 1, 5 and 3 lie in the region only at their corresponding minimum velocity value of 2m/s.

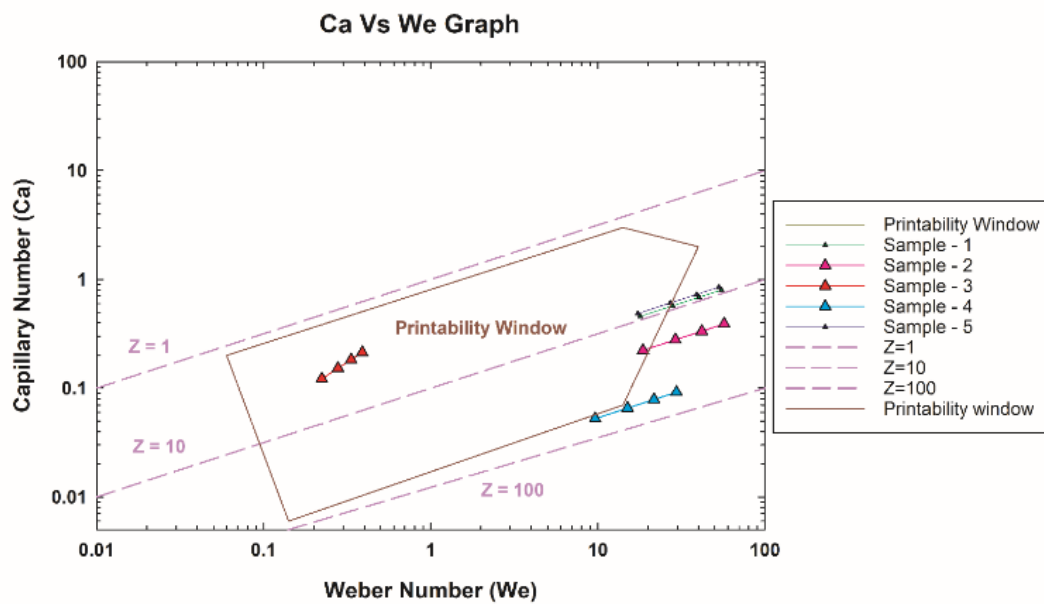


Fig.6 Ca vs We printability regime[13]

4. SIMULATION OF DROPLET FORMATION

To confirm the number of satellite and splashing of a droplet on the bed or substrate, drop formation simulation was performed in Flow 3D. This setup includes the same Pre-processing, designing, solving and post-processing steps. Simulation was done only for sample 1 and 5 because of their z range between 1 – 10.

4.1 Basic parameter input in Flow 3D

The basic input values are surface tension and dynamic viscosity. Surface tension values are given as 18g/s^2 for sample 1 and 19g/s^2 for sample 5 respectively. Similarly, Dynamic Viscosity values are given as 0.041 and 0.046 for sample 1 and 5. Finally, the density values are given as 1.010 and 1.030gm/cm^3 for sample 1 and 5 respectively. The contact angle is given as 90° according to standard values.

4.2 Modelling of nozzle, substrate and boundary condition

Under the model setup tab, there is a sub-tab called meshing and geometry which is useful to create the necessary nozzle, substrate and air boundary condition (Fig. 7.). A torus shape is selected to maintain the nozzle diameter as $50\mu\text{m}$ which is done by changing the values of major and minor radius of the Torus. The substrate is kept at a distance of 1mm from the nozzle. A cylindrical tank is also created so that it is capable of holding the ink. The cylindrical piston is created with a small thickness of $20\mu\text{m}$. A nozzle stopper is also given to make sure that the piston does not come out of the torus nozzle.

Finally, the meshing boundary surface is created slightly greater than the cylindrical tank to create an air boundary surface in the simulation as well as for the drop to flow through the 1mm or $1000\mu\text{m}$ air gap between the substrate and nozzle. In the output tab, the dynamic viscosity and distance travelled by the fluid is to be checked so that the software takes these 2 parameters into account. Under the numeric tab successive over-relaxation method is selected so that the errors can be reduced and the possibility for the solution to converge is increased.

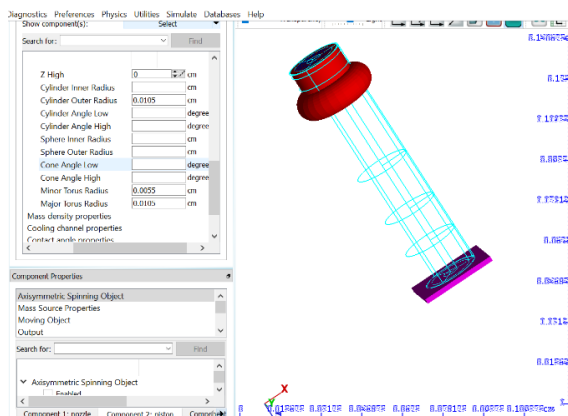


Fig. 6 Nozzle, ink tank, piston and substrate design

The substrate, cylinder and torus are fixed as static objects whereas the piston is set as moving objects and hence a velocity profile(Fig. 7.) have to be created such that the piston is capable of performing the work of a piezo-driven piston in binder jet printing.

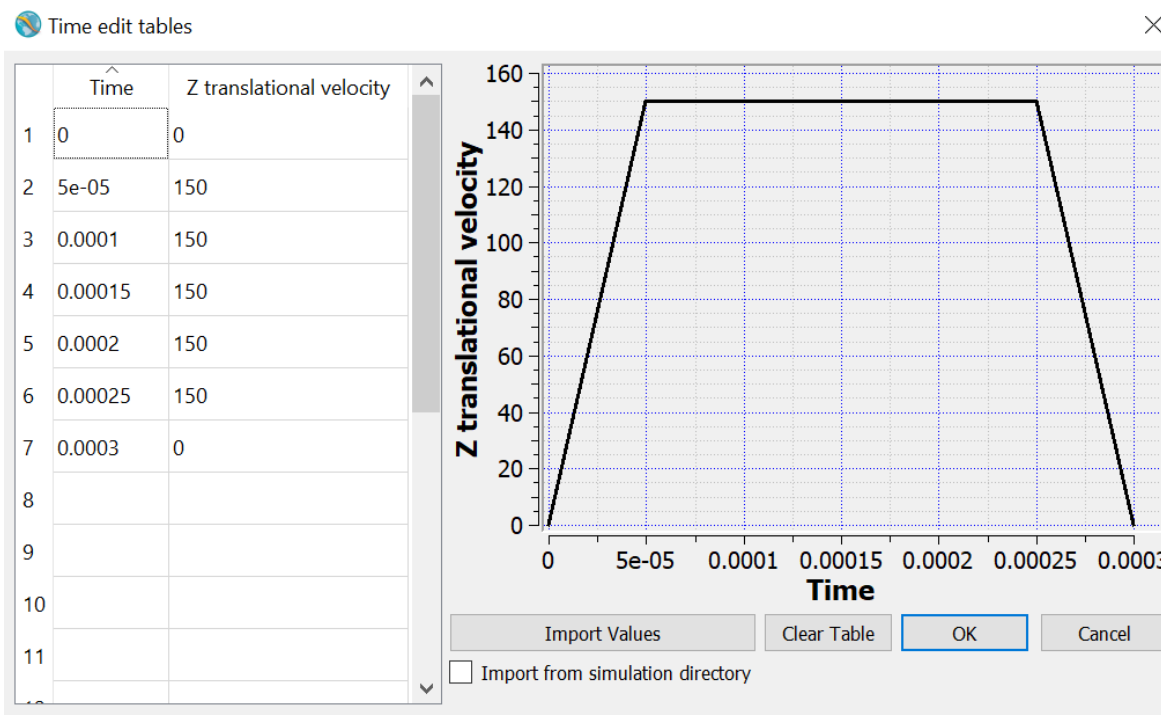


Fig. 7 Velocity profile for piston

Here the rise time is fixed as $1\mu\text{s}$ and the piston is in the full constant velocity of 1.5m/s for a time period of $250\mu\text{s}$ and finally the dwell or lowering time is kept as $1\mu\text{s}$ which is kept similar to the rise time [6].

4.3 Analysis

In this section pressure, velocity magnitude and 3D analysis of a drop was studied. Under contour variable, the necessary pressure or velocity is selected and simulated by selecting the X-Z plane. Horizontal symmetry is selected to study the full droplet formation by the droplet mechanism in air and hitting the surface.

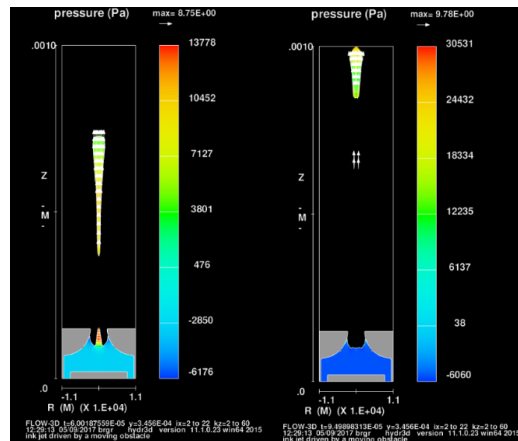


Fig. 7 Pressure Vector for sample – 1

The pressure vector is depicted in Fig. 7 where a clear drop formation and elongation of the droplet can be seen. The maximum velocity reached by droplet for sample 1 is 10m/s.

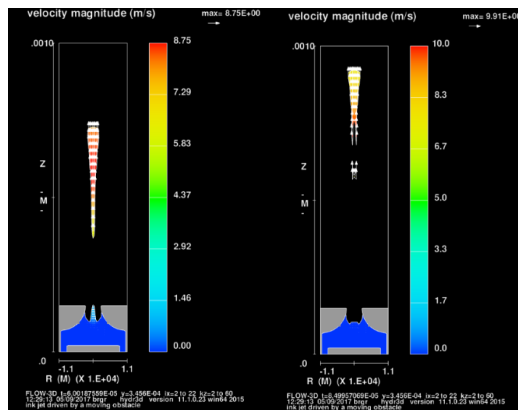


Fig. 8 Velocity magnitude vector for sample – 1

Figure 7 and 8 are for sample-1 wherein a single satellite formation can be identified from the existing elongated droplet, similarly, for sample-5 the pressure a velocity vector and magnitude graphs are in Fig. 9 and 10.

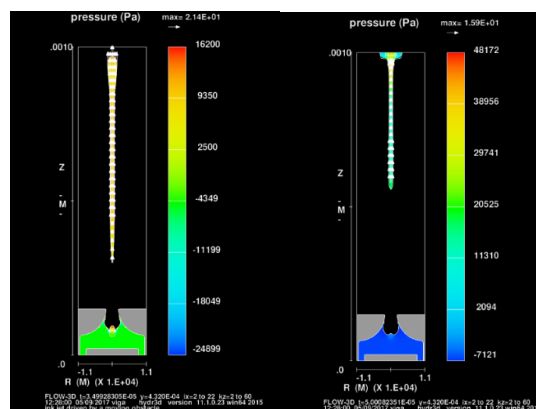


Fig. 9 Pressure vector for sample – 2

The maximum velocity reached for sample one and two are 11.3m/s and 26.4m/s whose outlet velocity can be controlled by controlling the velocity of the piston. Initially, the piston velocity is set as 1.5m/s.

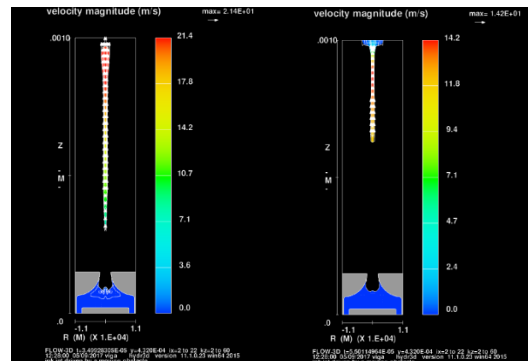


Fig. 10 Velocity magnitude vector for sample – 2

Whereas, the output velocity is increased about 10 times. This is an advantageous process through which we can increase the life of the piston and reduce the power consumed by the piezo-driven piston but should be controlled by tuning the voltage value so as to reduce the splashing of a droplet on the aluminium oxide nanoparticles.

5. RESULTS AND DISCUSSION

From the calculated dimensionless numbers, it is evident that the binder ejection should be done at a velocity above the minimum velocity to exceed the surface tension and viscous forces. Below this velocity, the binder is not appropriate for printing because of its high viscosity, splashing of satellite droplets, and inadequate energy for drop formation. It was observed that from Table 3, the values of Z for sample one and sample five is high because they have a rich concentration of Polyethylene glycol and less quantity of Isopropanol.

The highest minimum velocity value required is for sample four because it has less viscosity and requires greater pressure to reach such velocity to overcome the surface tension produced between the nozzle surface and ink surface. Whereas, the values for sample one and five will be less due to an increase in percentage contribution of additive than binder material.

From the above test and result values it was concluded that both polyethylene glycol and Isopropanol can be used for manufacturing any automotive components in binder jet printing but with a richer concentration of additive than binder because the tested values accept the Z value for sample one and five with additive and binder ratio of 3:1 and 4:1.

6. CONCLUSION

The material for additive, binder, and base metal is selected as Polyethylene glycol, Iso-Propanol and Aluminum Oxide nano-particles due to their effectively advantageous physical and mechanical properties. Therheological characteristics such as density, kinematic viscosity and surface tension were measured via both digital and mechanical instruments after performing sample preparation with the stir blending technique. Samples one and five have satisfied the boundary condition for printable parameter Z. This can be very effective cost-wise and as well as ink preparation time is also less. The only major demerit is that the

blended ink should be kept in a fully closed container as IsoPropanol is evaporative. When the composition of Polyethylene glycol is greater than IsoPropanol the binder is printable.

Finally, a graphical comparison and a simulation in Flow 3D software was to check the printability window, stable area, DOD printing regime and confirm the satellite formation characteristics. The corresponding velocity and pressure vector magnitude were also studied from the simulation. From this process, the synthesized ink can be used for binder jet printing for mass production of automotive components or manufacturing sand die which is used for casting process with good allowance and surface finish.

7. REFERENCES

- [1] Jiménez, M., Romero, L., Domínguez, I.A., Espinosa, M. d. M., and Domínguez, M., (2019). "Additive Manufacturing Technologies: An Overview about 3D Printing Methods and Future Prospects," *Complexity*, 2019, 1-30, doi: 10.1155/2019/9656938.
- [2] Pérez, M., Carou, D., Rubio, E. M., and Teti, R., (2019). "Current Advances in Additive Manufacturing," *Procedia CIRP*, 88, 439-444, doi: 10.1016/j.procir.2020.05.076
- [3] Carneiro, O. S., Silva, A. F., and Gomes, R., (2015). "Fused deposition Modeling with Polypropylene," *Materials & Design*, 83, 768-776, doi: 10.1016/j.matdes.2015.06.053
- [4] Dini, F., Ghaffari, S. A., Jafar, J., Hamidreza, R., and Marjan, S., (2020). "A Review of Binder Jet Process Parameters; Powder, Binder, Printing and Sintering Condition," *Metal Powder Report*, 75(2), 95-100, doi: 10.1016/j.mprp.2019.05.001
- [5] Lv, X., Ye, F., Cheng, L., Fan, S., and Liu, Y., (2019). "Binder Jetting of Ceramics: Powders, Binders, Printing Parameters, Equipment, and Post-treatment," *Ceramics International*, 45(10), 12609-12624, doi: 10.1016/j.ceramint.2019.04.012
- [6] Zhao, H., Ye, C., Xiong, S., Fan, Z., and Zhao, L., (2020). "Fabricating an Effective Calcium Zirconate layer over the Calcium Grains via Binder-jet 3D-Printing for Improving the Properties of Calcium Ceramic Cores," *Additive Manufacturing*, 32, doi: 10.1016/j.addma.2019.101025
- [7] Ziaee, M., and Crane, N. B., (2019). "Binder jetting: A review of Process, Materials, and Methods," *Additive Manufacturing*, 28, 781-801, doi: 10.1016/j.addma.2019.05.031
- [8] Miyanaji, H., (2019). "Binder Jetting Additive Manufacturing Process Fundamentals and the Resultant Influences on Part Quality," doi: 10.18297/etd/3058
- [9] Prasad, P. S. R. K., Reddy, A. V., Rajesh, P.K., Ponnambalam, P., and Prakasan, K., (2006). "Studies on Rheology of Ceramic Inks and Spread of Ink Droplets for Direct Ceramic Ink Jet Printing," *Journal of Materials Processing Technology*, 176(1-3), 222-229, doi: 10.1016/j.jmatprotec.2006.04.001
- [10] Jain, S.; Palia, A. Opportunities and Challenges in Paper Printed RFID. *IARS' International Research Journal*, Vic. Australia, v. 7, n. 2, 2017. DOI: 10.51611/iars.irj.v7i2.2017.82.
- [11] Derby, B., (2010). "Inkjet Printing of Functional and Structural Materials: Fluid Property Requirements, Feature Stability, and Resolution," *Annual Review of Materials Research*, 40(1), 395-414, doi: 10.1146/annurev-matsci-070909-104502
- [12] Kang, S., Kim, S., and Sohn, D. K., and Ko, H.S., (2020). "Analysis of Drop-on-Demand Piezo Inkjet Performance," *Physics of Fluids*, 32(2), doi: 10.1063/1.5142023
- [13] Koivunen, R., Bollström, R., and Gane, P., (2020). "Inkjet Jetability and Physical Characterization of Water-ethanol Solutions of Low Molecular Weight Sodium Polyacrylate and Poly-diallyl Dimethyl Ammonium Chloride (polyDADMAC)," *AIP Advances*, 10(5), doi: 10.1063/5.0006634

- [14] Kiaee, M. M., Maeder, T., and Brugger, J., (2020). "Inkjet-Printed Composites for Room-Temperature VOC Sensing: From Ink Formulation to Sensor Characterization," *Advanced Materials Technologies*, 6(1), doi: 10.1002/admt.202000929
- [15] Sim, W., Park, S., Park, C., Yoo, Y., Kim, Y., Joung, J., and Oh, Y., (2006). "Analysis of the Droplet Ejection for Piezoelectric-driven Industrial Inkjet Head, " *NSTI-Nanotech*, 528-533.
- [16] Jain, H. "Scope of Energy Conservation in Pumping System", *IARS' International Research Journal. Vic. Australia*, 10(2) 2020. doi: 10.51611/iars.irj.v10i2.2020.105.